

## THERMAL ANALYSIS OF FLAMMABILITY

R. E. Lyon\*, R. N. Walters, and S. I. Stoliarov<sup>1</sup>

Airport and Aircraft Safety Research and Development Division, Fire Safety Branch, Federal Aviation Administration  
W. J. Hughes Technical Center, Atlantic City International Airport, NJ 08405, USA

<sup>1</sup>SRA International, 3120 Fire Road, Egg Harbor Township, NJ 08405, USA

A thermal analysis method that separately reproduces the gas and condensed phase processes of flaming combustion in a single laboratory test is described. Anaerobic pyrolysis of solid plastics at a constant heating rate and complete thermal oxidation (nonflaming combustion) of the evolved gases provides the rate, amount, and temperatures over which heat is released by a burning solid. A physical basis for the method, the test procedure, and the relationship of flammability parameters to fire response and flame resistance of plastics are described.

**Keywords:** combustion, flammability, polymer

### Introduction

A considerable amount of effort has been expended to relate laboratory thermal analyses to polymer flammability [1, 2 and references therein]. The motivation for these studies is the desire for quantitative data to use in materials design and evaluation and the convenience of testing milligram-sized samples under controlled laboratory conditions. The present approach separately reproduces the gas and condensed phase processes of flaming combustion in a single laboratory test using controlled heating and complete combustion of the evolved fuel gases in excess oxygen. In this way, the normally coupled process of condensed phase fuel generation and gas phase flaming combustion are decoupled and forced to completion so that the maximum potential of the sample to release heat by burning is obtained in a reproducible test.

### Models

#### Condensed phase model

The mass loss/fuel generation rate of a polymer at a burning surface can be described by single-step, first-order thermal decomposition kinetics [1]

$$-\frac{dm}{dt} = k_p(m - m_c) = k_p(m - \mu m_0) \quad (1)$$

where  $m$  is the instantaneous mass of polymer,  $m_c$  is the mass of char remaining after pyrolysis,  $m_0$  is the initial mass, and  $\mu = m_c/m_0$  is the constant mass

fraction of char. The rate constant for thermal decomposition at temperature  $T$  is

$$k_p = A \exp\left[-\frac{E_a}{RT}\right] \quad (2)$$

in terms of the frequency factor  $A$ , global activation energy  $E_a$ , and gas constant  $R$ . If the sample is thermally decomposed at a constant heating rate  $dT/dt = \beta$ , the independent variable is transformed from time to temperature, and Eq. (1) can be integrated to give the fraction of the initial mass remaining at temperature  $T$  [1],

$$\frac{m(T)}{m_0} = \mu + (1 - \mu)e^{-y} \quad (3)$$

where the exponent  $y = (ART^2 \exp[-E_a/RT]) / \beta(E_a + 2RT)$  has complex temperature dependence. The specific mass loss rate at temperature  $T$  for a constant heating rate  $\beta$  is the time derivative of Eq. (3),

$$\frac{-1}{m_0} \frac{dm}{dt} = (1 - \mu)k_p e^{-y} \quad (4)$$

Equation (4) has a maximum value for  $\mu \neq 1$  [1],

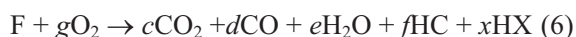
$$-\frac{1}{m_0} \frac{dm}{dt} = \frac{\beta(1 - \mu)}{eRT_{\max}^2/E_a} = \frac{\beta(1 - \mu)}{\Delta T_p} \quad (5)$$

where  $T_{\max}$  is the temperature at maximum mass loss/fuel generation rate,  $e$  is the natural number, and  $\Delta T_p = eRT_{\max}^2/E_a$  is the characteristic temperature interval over which pyrolysis occurs [1, 2].

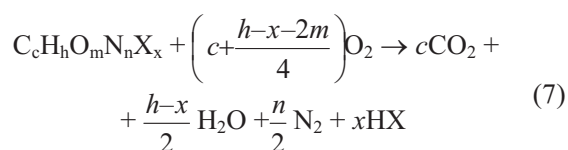
\* Author for correspondence: richard.e.lyon@faa.gov

*Gas phase model*

The reaction of volatile fuel F with oxygen in the gas phase can yield complete (CO<sub>2</sub>, H<sub>2</sub>O, HX) and incomplete (CO, HC) combustion products depending on the conditions, i.e.,



where X is a halogen, HX is a halogen acid, and HC is a gaseous hydrocarbon. If there is sufficient time, temperature, and oxygen for complete combustion, then  $d=f=0$  and the amount of oxygen consumed by combustion is defined by the fuel composition,  $F = C_cH_hO_mN_nX_x$ ,



The stoichiometric oxygen/fuel mass ratio  $r_0$  is readily calculated from Eq. (7) for fuels of known composition and is in the range  $r_0 = 2.0 \pm 1.5$  for the majority of organic compounds [3]. Thornton [4] was the first to notice that the heat of complete combustion of organic gases and liquids  $h_{c,v}^0$  (J/g-fuel) divided by the stoichiometric mass ratio was essentially constant and independent of the type of fuel

$$C = h_{c,v}^0 / r_0 = 13.1 \pm 0.7 \text{ kJ/g-O}_2 \quad (8)$$

This observation was extended to solids by Huggett [5] and became the basis for oxygen consumption calorimetry [6], whereby measurement of the mass of oxygen consumed from the combustion atmosphere is used to deduce the amount of heat released during the burning of plastics and products [7, 8]. Equation (8) is valid only for complete combustion, i.e., Eq. (7).

Multiplying the specific mass loss rate of a thermally decomposing solid by the heat of combustion of the evolved gases  $h_{c,v}^0$ , assuming complete combustion, and invoking the oxygen consumption principle Eq. (8) gives the specific heat release rate (W/g-sample) by oxygen consumption [9]

$$Q(t) = \frac{-h_{c,v}^0}{m_0} \frac{dm}{dt} = -\frac{C}{m_0} \frac{dr_0m}{dt} = \frac{\rho CF}{m_0} [\Delta O_2](t) \quad (9)$$

In Eq. (9),  $\rho$  and  $F$  are the oxygen density and volumetric flow rate of the gas stream, respectively, and  $[\Delta O_2](t)$  is the change in the volume fraction of oxygen in the gas stream due to combustion at time,  $t$ . The specific heat of combustion of the sample is the time integral of  $Q(t)$

$$h_c^0 = (1-\mu)h_{c,v}^0 = \int_0^\infty Q(t)dt = \frac{\rho C}{m_0} \int_0^\infty F[\Delta O_2](t)dt \quad (10)$$

If the sample is small ( $\approx 5$  mg) and heated at a constant rate of temperature rise  $\beta$  such that thermal equilibrium with the heat source is maintained, then according to Eqs (5), (9), and (10), the maximum value of the specific heat release rate in terms of oxygen consumption is

$$Q_{\max} = \frac{-h_{c,v}^0}{m_0} \frac{dm}{dt} \Big|_{\max} = \frac{\beta h_c^0}{\Delta T_p} = \frac{\rho CF}{m_0} [\Delta O_2]_{\max} \quad (11)$$

Dividing Eq. (11) by  $\beta$  yields a flammability parameter with the units and significance of a heat release capacity [1, 2]

$$\eta_c = \frac{Q_{\max}}{\beta} = \frac{h_c^0}{\Delta T_p} = \frac{\rho CF}{\beta m_0} [\Delta O_2]_{\max} \quad (12)$$

The heat release capacity  $\eta_c$  is comprised of thermal stability and combustion properties ( $h_c^0$ ,  $\mu$ ,  $E_a$ ,  $T_{\max}$ ) and is measurable by oxygen consumption calorimetry [9].

## Experimental

### Materials

All plastics tested were unfilled, natural, or virgin-grade resins or blends obtained from Aldrich Chemical Company, Scientific Polymer Products, or directly from manufacturers. Methane, oxygen, and nitrogen gases used for calibration and testing were dry, ultrahigh purity grades obtained from Matheson Gas Products.

### Methods

#### Combustion kinetics of gas phase

Oxygen consumption was used to study the thermal oxidation kinetics of typical fuel gases to determine the time-temperature requirements for complete combustion of polymer pyrolysis products under laboratory conditions. The apparatus used in these experiments has been described previously [9] and consists of a pyrolysis probe in a heated manifold attached to a 5-m-long Inconel combustion tube having an inner diameter of 4.5 mm, which is coiled to fit inside of a ceramic furnace. In the experiments, the fuel concentration was constant, oxygen was present in large excess, and the residence time (flow rate) of the gases and the temperature of the combustor were independently varied in stepwise increments of 50 cm<sup>3</sup> min<sup>-1</sup> between flow rates of 50–200 cm<sup>3</sup> min<sup>-1</sup> and in 10°C increments between combustor temperatures of 500°C–1000°C. Fuel gases were methane (4% by vol. in air), the volatile pyrolysis products of poly-

methylmethacrylate/PMMA (methylmethacrylate monomer), and the pyrolysis products of polypropylene/PP (alkanes and alkenes). The combustion stream was analyzed for residual oxygen to compute the extent of reaction for each residence time and combustor temperature. The residence time for complete (99.5%) thermal oxidation of polymer pyrolysis products was estimated from oxygen consumption using pseudo first-order reaction kinetics [9–11].

Pyrolysis-combustion flow calorimetry (PCFC)

Figure 1 is a flow diagram of the pyrolysis combustion flow calorimeter (PCFC) that illustrates how the condensed phase (pyrolysis) and gas phase (combustion) processes of flaming combustion are separately reproduced in a nonflaming test. Figure 2 is a schematic drawing of the PCFC. In the test, a 1–10 milligram sample mass  $m_0$  is weighed into a ceramic cup, inserted and sealed into the pyrolyzer, and heated at a constant rate of temperature rise ( $1 \text{ K s}^{-1}$ , typically) to  $900^\circ\text{C}$ . During sample heating, the volatile thermal

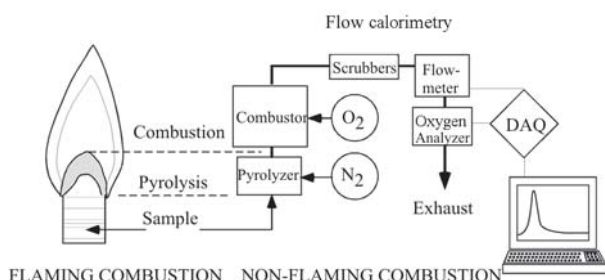


Fig. 1 Component processes of flaming combustion and PCFC. Processes are decoupled in PCFC and forced to completion

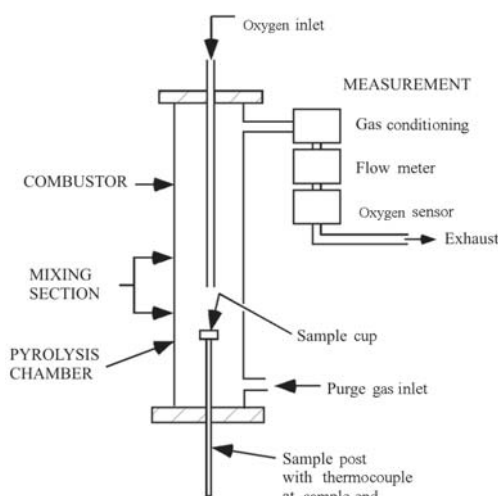


Fig. 2 Schematic diagram of the PCFC

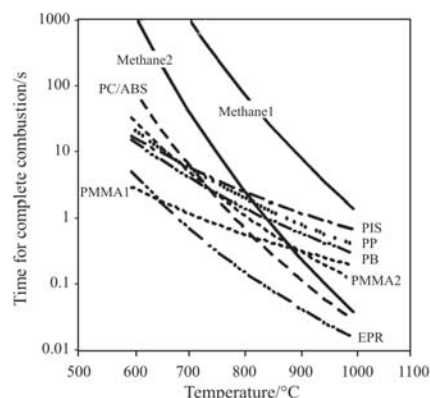


Fig. 3 Time-temperature curves for 99.5% combustion of various fuel gases

decomposition products are swept from the pyrolyzer by an inert gas (typically nitrogen) and mixed with excess oxygen prior to entering a  $900^\circ\text{C}$  combustor for 10 s (see Results/Combustion Kinetics and Fig. 3 which follows) to effect complete oxidation of the decomposition products. The combustion gas stream is scrubbed to remove water and acid gases prior to entering a mass flow meter and oxygen analyzer. The heat release capacity is the maximum value of the specific heat release rate measured during the experiment divided by the heating rate,  $\eta_c = Q_{\max}/\beta$ . The total heat release  $h_c^0$  is the time integral of the specific heat release rate over the entire duration of the experiment, i.e., Eq. (10). The heat release temperature  $T_{\max}$  is the sample temperature at  $Q_{\max}$ . The sample is weighed after the test to determine the residual mass  $m_c$ , and the char yield is calculated,  $\mu = m_c/m_0$ .

Results and discussion

Combustion kinetics

The results of the combustion kinetics experiments and calculations are shown in Fig. 3 for methane (methane1), PP, and PMMA (PMMA1) data obtained in our laboratory and literature data for methane (methane2) [10], as well as PMMA (PMMA2), polybutadiene/PB, polyisoprene/PIS, ethylene-propylene rubber/EPR, and a polycarbonate/ acrylonitrile-butadiene-styrene (PC/ABS) blend [11]. It is clear from Fig. 3 that thermal oxidation of hydrocarbon fuels in excess oxygen is 99.5% complete in 10 s at  $900^\circ\text{C}$ .

Pyrolysis-combustion flow calorimetry

Figure 4 shows experimental data for the reduced heat release rate  $Q/\beta$  vs. temperature for polyoxymethylene (POM), PMMA, polyvinylchloride (PVC), polyethyleneterephthalate (PET), polyamide 66 (PA66),

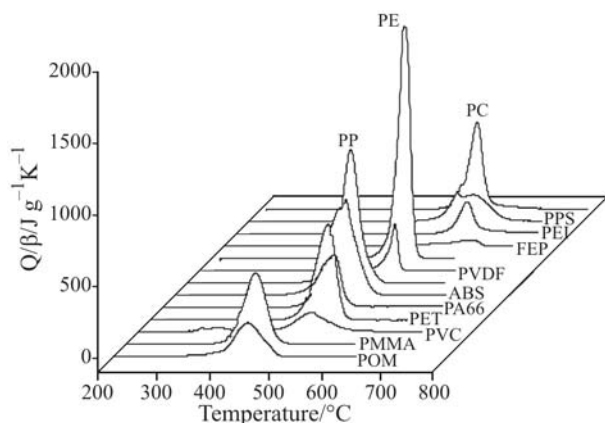


**Fig. 4** Heat release histories for 13 common polymers in the PCFC

ABS, polypropylene (PP), polyvinylidene fluoride (PVDF), polyethylene (PE), fluorinated ethylene-propylene (FEP), polyether-imide (PEI), polyphenylene-sulfide (PPS), and polycarbonate (PC) measured by PCFC at a heating rate of 1 K s<sup>-1</sup> using a combustor residence time of 10 s at 900°C. The data in Fig. 4 shows that  $Q_{max}/\beta = \eta_c$  varies widely in magnitude and temperature for common polymers.

Figure 5 compares the heat release capacity  $\eta_c$  of 15 polymers obtained by PCFC at  $\beta=4$  K/s to  $\eta_c$  obtained with a thermal gravimetric analyzer (TGA) at a heating rate of 0.17 K/s connected to a gas chromatograph (GC) and mass spectrometer (MS) [12] to analyze the pyrolysis gases and calculate their heats of combustion. The average difference between the heat release capacities by the two different techniques is 13%, which is comparable to the inherent variability of the TG-GC/MS methodology. Table 1 lists the flammability parameters measured in a single 15-min PCFC test, including the heat release capacity  $\eta_c$ , the total heat released, the char yield  $\mu$ , and the sample temperature at peak heat release rate  $T_{max}$  for the polymers in Fig. 4. The average intra-

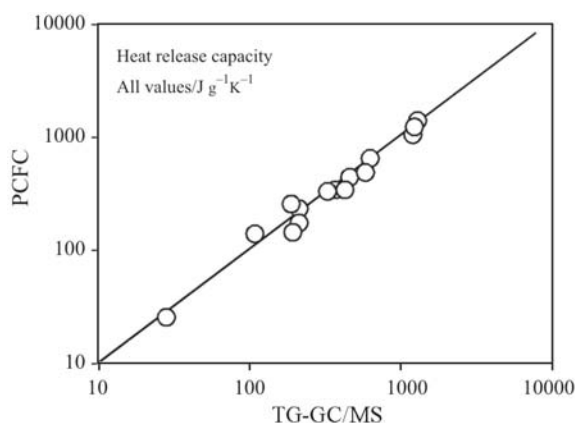


**Fig. 5** Comparison of PCFC and TGA-GC/MS data for  $\eta_c$  (15 plastics)

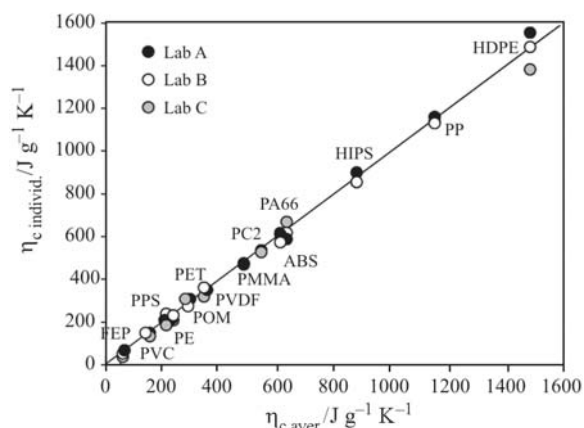


**Fig. 6** Comparison of individual and average values of  $\eta_c$  obtained by three laboratories

**Table 1** Flammability parameters of common polymers from PCFC (triplicate determinations)

POLYMER	$\eta_c^0$ / J g <sup>-1</sup> K <sup>-1</sup>	$h_c^0$ / kJ g <sup>-1</sup>	$\mu$ / %	$T_{max}$ / °C
HDPE	1486±20	43.5±0.1	0.1±0.1	504±1
PP	1130±24	43.2±0.2	0.0±0.0	483±1
HIPS	859±4	37.8±0.1	2.5±0.2	452±1
PA66	623±34	29.4±0.1	1.0±0.1	475±2
ABS	581±14	37.0±0.2	6.2±0.3	454±1
PC 2	539±26	20.4±0.2	22.5±0.8	547±2
PC 1	484±13	20.4±0.1	23.2±0.2	545±3
PMMA	475±6	24.9±0.1	0.0±0.0	393±2
PET	357±16	16.8±0.7	12.6±1.5	459±3
PVDF	334±38	7.8±1.1	16.4±3.5	509±4
POM	267±19	16.2±0.0	0.0±0.0	398±6
PPS	248±27	15.7±0.1	44.0±0.6	535±1
PEI	201±7	9.3±0.2	51.3±0.3	565±1
PVC	129±3	10.8±0.2	18.8±0.1	467±4
FEP	57±1	4.1±0.0	0.0±0.0	589±1

laboratory variability (coefficient of variation) of a particular sample parameter in the PCFC is less than 5%. Figure 6 is a plot of the heat release capacities of the polymers in Table 1 obtained by three different laboratories compared to the average value of  $\eta_c$  for the three laboratories. The interlaboratory variability (coefficient of variation) is about 10%, which is comparable to the variation between manufacturers (compare PC 1 and PC 2 in Table 1).

### Correlation of PCFC with flammability

#### Ignitability

The critical heat flux for sustained ignition CHF is a measure of the ignition resistance of a material and



determines the ease with which it becomes involved in a fire. For piloted ignition,  $\text{CHF} \approx \sigma T_{\text{ign}}^4$ , where  $\sigma$  is the Boltzmann radiation constant,  $T_{\text{ign}}$  the ignition temperature of the material, and CHF is the heat flux lost from the surface by radiation and convection to the surroundings. Since  $T_{\text{ign}} \approx T_{\text{max}}$ , the CHF estimated from PCFC data is [13–16],

$$\text{CHF} \approx \sigma T_{\text{max}}^4 \quad (13)$$

Table 2 lists average  $T_{\text{max}}$  for 14 polymers obtained from three different laboratories whose  $\eta_c$  data is plotted in Fig. 6. Also listed in Table 2 are the CHF calculated from  $T_{\text{max}}$  using Eq. (13) and measured CHF for these polymers [13]. Reasonable agreement is observed between the CHF estimated from  $T_{\text{max}}$  and the CHF measured directly for hydrocarbon polymers. For heteroatom (PPS) and halogen-containing (PVC, PVDF, FEP) polymers with low  $h_c^0$ , Eq. (13) underestimates CHF because  $T_{\text{ign}} > T_{\text{max}}$  [13, 15] and heat release rate is a better predictor of sustained ignition (see Flame Resistance) [16].

### Fire response

The single best parameter characterizing the fire hazard of a polymer is its heat release rate HRR ( $\text{W m}^{-2}$ ) in flaming combustion [17]. However, HRR is difficult to quantify in fire calorimeters because the test results depend on the external heat flux (heating rate), sample thickness, sample orientation, edge conditions, ventilation rate, etc. In contrast, the heat release capacity measured by PCFC using controlled pyrolysis and complete combustion of the fuel gases

depends only on the material being tested. The heat release rate of a solid polymer in flaming combustion is characterized by a heat of gasification  $L_g$  and an effective heat of combustion of the fuel gases HOC, which is related to  $h_{c,v}^0$  by the combustion efficiency in the flame,  $\chi = \text{HOC}/h_{c,v}^0$ . The driving force for HRR is the difference between the heat influx from the flame ( $q_{\text{flame}}''$ ) and any external sources ( $q_{\text{ext}}''$ ) and the heat losses from the surface  $q_{\text{loss}}''$ .

$$\text{HRR} = \chi \frac{h_{c,v}^0}{L_g} (q_{\text{flame}}'' - q_{\text{loss}}'' + q_{\text{ext}}'') \quad (14)$$

The HRR in flaming combustion Eq. (14) assumes a linear form [13–15] with respect to the independent variable  $q_{\text{ext}}''$

$$\text{HRR} = \text{HRR}_0 + \text{HRP} q_{\text{ext}}'' \quad (15)$$

In Eq. (15),  $\text{HRP} = \chi h_{c,v}^0 / L_g$  is the dimensionless heat release parameter for flaming combustion and  $\text{HRR}_0 = \text{HRP} (q_{\text{flame}}'' - q_{\text{loss}}'')$  is the limiting heat release rate at zero external heat flux. According to Eq. (12),  $\eta_c = h_c^0 / \Delta T_p$ , so the heat release parameter can be written

$$\text{HRP} \equiv \chi \frac{h_{c,v}^0}{L_g} = \chi \frac{h_c^0 / \Delta T_p}{h_g / \Delta T_p} = \frac{\eta_c}{\eta_g} \quad (16)$$

where,  $\eta_g = h_g / \chi \Delta T_p$  is a normalizing parameter, where  $h_g$  is the heat of gasification per unit initial mass of solid. When,  $q_{\text{ext}}'' \gg q_{\text{flame}}'' - q_{\text{loss}}''$ , then according to Eqs (14)–(16) the heat release rate is

$$\text{HRR} = \text{HRR}_0 + \text{HRP} q_{\text{ext}}'' \approx \text{HRP} q_{\text{ext}}'' \approx \eta_c \frac{q_{\text{ext}}''}{\eta_g} \quad (17)$$

At an external heat flux  $q_{\text{ext}}'' = 50 \text{ kW m}^{-2}$  typical of a large fire,  $\text{HRR}_0 < \text{HRP} q_{\text{ext}}''$ . Under these conditions for typical polymers having  $\eta_g = h_g / \chi \Delta T_{p,0} \approx (2 \text{ MJ kg}^{-1}) / ((0.8)(50 \text{ K})) = 50 \text{ kJ kg}^{-1} \text{ K}$ , Eq. (17) predicts

$$\text{HRR} = \frac{q_{\text{ext}}''}{\eta_c} \eta_c \approx \frac{50 \text{ kW m}^{-2}}{50 \text{ kJ kg}^{-1} \text{ K}} \eta_c = 1 \frac{\text{kg-K}}{\text{m}^2 \text{-s}} \eta_c$$

In other words, the HRR in flaming combustion at high external heat flux should be roughly proportional to  $\eta_c$  with slope  $1 \text{ kg-K/m}^2\text{-s}$  at  $q_{\text{ext}}'' = 50 \text{ kW m}^{-2}$ . Figure 7 is a plot of the peak HRR in flaming combustion measured in a fire calorimeter at  $q_{\text{ext}}'' = 50 \text{ kW m}^{-2}$  according to a standard method [7] vs.  $\eta_c$  measured in the PCFC for the same or similar polymers. The solid line through the data has the expected slope  $1 \text{ kg-K/m}^2\text{-s}$  and describes the trend reasonably well considering it represents an average value of  $\eta_g$ . Figure 8 is a plot of the maximum (peak) value of the HRR measured in a fire calorimeter that operates on the sensible enthalpy method [18] vs. the heat release capacity  $\eta_c$  of the same material. The horizontal

**Table 2** Critical heat fluxes calculated from  $T_{\text{max}}$  and measured in a fire calorimeter

Polymer	$T_{\text{max}}/^\circ\text{C}$	CHF, $\text{kW m}^{-2}$	
		Eq. (13)	Measured [13]
PMMA	401±8	11–12	6–23
POM	409±10	11–13	13
HIPS	463±10	15–17	15
ABS	467±12	16–18	9–15
PET	471±12	16–18	10–19
PA66	482±11	17–19	15–21
PVC	478±8	17–18	15–28
PP	493±10	18–20	15–16
PE	514±10	20–22	15–20
PVDF	510±2	21	30–50
PC	556±9	25–28	15–20
PPS	551±18	24–28	35–38
PEI	576±10	28–31	25–40
FEP	600±10	31–34	28–50

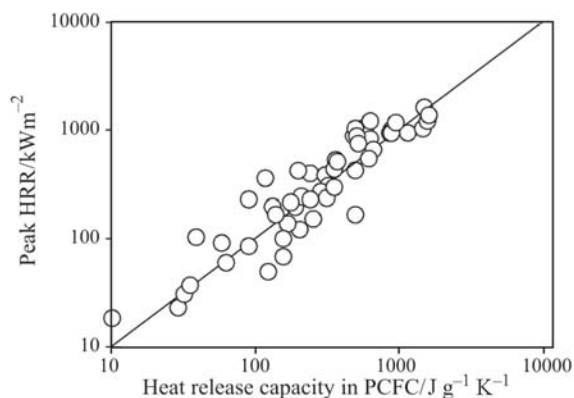


**Fig. 7** Peak heat release rate in cone calorimeter at 50 kW m<sup>-2</sup> external flux vs. heat release capacity in PCFC

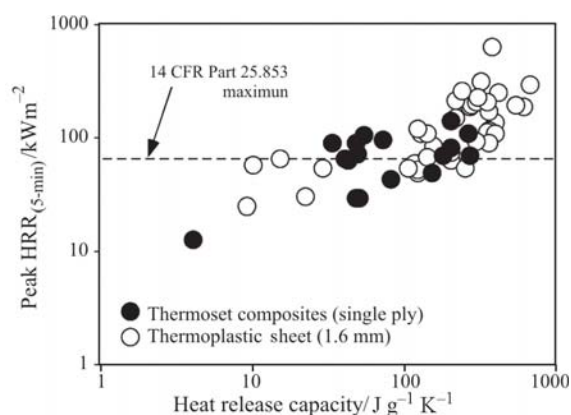


**Fig. 8** Peak HRR in 14 CFR 25.853 vs. heat release capacity in PCFC

dashed line at HRR=65 kW m<sup>-2</sup> is the maximum HRR allowed by the Code of Federal Regulations Part 25 during the standard 5-min test [19] required of large-area materials in commercial aircraft cabins. In general, it is seen that peak HRR for these thin (1–3 mm) materials increases with  $\eta_c$ , and the data is roughly approximated by a power law,  $HRR (kW m^{-2}) = 8\eta_c^{1/2}$  with a correlation coefficient  $R=0.64$ .

### Flame resistance

Flame resistance is an aspect of flammability that relates to the tendency of a thin strip of material to cease burning after brief ignition by a small flame such as a Bunsen burner. The two most popular flame resistance tests are considered here – the limiting oxygen index test LOI [20] and the Underwriters Laboratory test for flammability of plastic materials UL 94 [21]. In the latter (UL 94), the time to extinction of the sample flame after removal from a Bunsen burner flame is measured under ambient conditions. At the start of the test the Bunsen burner is removed so that  $q''_{ext} = 0$  at  $t=0$ . If a minimum (critical) heat release rate  $HRR^*$  is required to sustain flaming combustion [13–15,

22, 23] then according to Eqs (15) and (16) flame extinction in the UL test should occur when

$$HRR(q''_{ext}=0) = HRR_0 = \frac{\eta_c}{\eta_g} (q''_{flame} - q''_{loss}) \leq HRR^* \quad (18)$$

For upward burning in air  $HRR^* \approx 50 \text{ kW m}^{-2}$  [22], and with  $q''_{flame} \approx 30 \text{ kW m}^{-2}$  [24] and  $q''_{loss} \approx CHF \approx 17 \text{ kW m}^{-2}$  (Table 2) the extinction condition (Eq. (18) becomes

$$\eta_c \leq \frac{\eta_g HRR^*}{q''_{flame} - q''_{loss}} \approx \frac{(50 \text{ kJ/kg} - K)(50 \text{ kW/m}^2)}{(30 \text{ kW/m}^2 - 17 \text{ kW/m}^2)} \approx 200 \text{ J g}^{-1} \text{ K}^{-1} \quad (19)$$

Figure 9 compares UL 94 vertical test results for plastics to the heat release capacity ( $\eta_c$ ) measured in the PCFC for compositions spanning a wide range of chemical structure and thermal stability. Figure 9 shows that a transition from sustained burning (no vertical rating/NR) to self-extinguishing (V0) occurs at roughly  $\eta_c = 200 \text{ J/g-K}$  as predicted by Eq. 19.

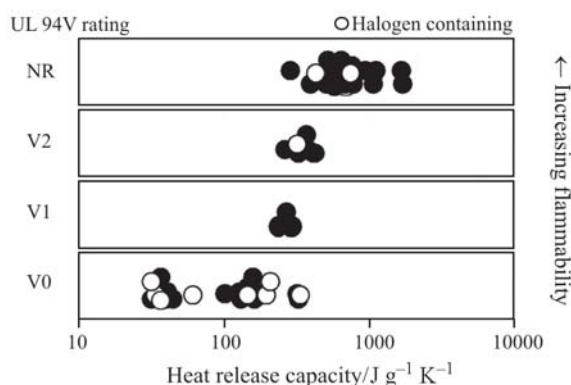


**Fig. 9** UL 94 V rating vs. heat release capacity of polymers (NR=no rating in vertical test)

In the limiting oxygen index (LOI) test the same initial conditions apply as in the UL 94 test (i.e.,  $q''_{ext} = 0$  at  $t=0$ ) but the volume fraction of oxygen in the test chamber  $[O_2]$  is adjusted until flame extinction occurs. Since [24],  $q''_{flame} \propto [O_2] = a[O_2]$ , Eq. (18) predicts that flame extinction occurs in the LOI test when

$$\eta_c \leq \frac{\eta_g HRR^*}{q''_{flame} - q''_{loss}} = \frac{\eta_g HRR^*}{a[O_2] - q''_{loss}}$$

or at a critical oxygen fraction

$$LOI = [O_2]^* = \frac{q''_{loss}}{a} + \frac{\eta_g HRR^*/a}{\eta_c} \quad (20)$$

Surface heat losses are of the order  $q''_{loss} = CHF \approx 17 \text{ kW m}^{-2}$  and the critical heat release rate for downward burning in the LOI test is  $HRR^* \approx 100 \text{ kW m}^{-2}$  [13, 22]. Empirically it is found

[24] that  $a=1.40 \text{ kW/m}^2\text{-}\%[\text{O}_2]$ , so the oxygen concentration at extinction  $[\text{O}_2]^*=\text{LOI}$  from Eq. (20) is

$$\text{LOI} = \frac{17 \text{ kW m}^{-2}}{1.4 \text{ kW m}^{-2} - \% [\text{O}_2]} + \frac{(50 \text{ kJ/kg-K})(100 \text{ kW m}^{-2})/(1.4 \text{ kW m}^{-2} - \% [\text{O}_2])}{\eta_c}$$

or

$$\text{LOI}(\%) = 12 + \frac{4 \text{ kJg}^{-1} \text{ K}^{-1}}{\eta_c} \quad (21)$$

Figure 10 is a plot of LOI vs.  $\eta_c$  for polymers of the same or similar composition. The solid line is Eq. (21), which provides a reasonable correlation of the data for both hydrocarbon and halogen-containing polymers.

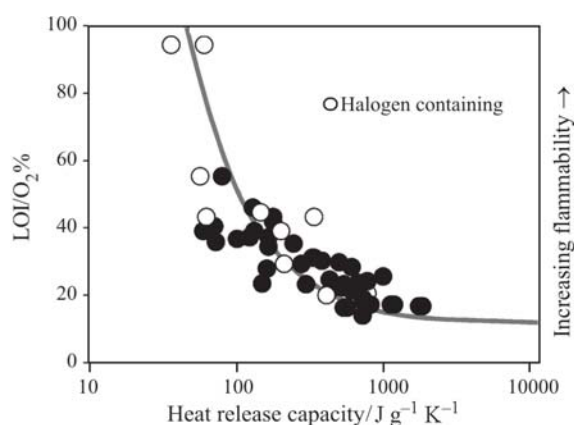


**Fig. 10** Limiting oxygen index (LOI) vs. heat release capacity of polymers. Solid line through data is Eq. (21)

Eqs (18)–(21) and Figs. 9 and 10 show that  $\eta_c$  is a good predictor of flame test results because self-extinction in these tests is a critical phenomenon that occurs at a particular HRR and consequently, a particular value of  $\eta_c$  [13–15]. Four regimes of flammability can be distinguished from Figs 8–10 for pure polymers:

- $\eta_c \geq 400 \text{ J g}^{-1} \text{ K}^{-1}$ ; No vertical rating (NR) in the UL 94 vertical burn test and  $\text{LOI} < 25$ .
- $\eta_c = 200\text{--}400 \text{ J g}^{-1} \text{ K}^{-1}$ ; Transient ignition in UL test (V2/V1) and  $\text{LOI} = 25\text{--}30$ .
- $\eta_c = 100\text{--}200 \text{ J g}^{-1} \text{ K}^{-1}$ ; Self extinguishing in UL test (V0/5V) and  $\text{LOI} = 30\text{--}40$ .
- $\eta_c \leq 100 \text{ J g}^{-1} \text{ K}^{-1}$ ; No ignition (no after-flame in UL test) and  $\text{LOI} > 40$ . These materials usually (e.g., Fig. 8) pass strict Federal Aviation Administration requirements [19] for the heat release rate of materials used in commercial aircraft cabins [14].

## Conclusions

A thermal analysis method for laboratory determination of flammability parameters of materials is presented. The method separately reproduces the condensed phase (pyrolysis) and gas phase (oxidation) processes of flaming combustion in a single, non-flaming combustion test. Decoupling the pyrolysis and combustion processes in this way, and forcing them to completion, isolates the thermochemistry of the condensed phase and provides the maximum potential (capacity) of the material to release heat in fires. A simple burning model with a critical heat release rate for extinction provides a physical basis for the observed correlation between flammability tests and the results of PCFC. Physical and chemical phenomena such as melting, dripping, heat distortion, swelling, charring, intumescence and incomplete combustion are not captured by milligram samples in the PCFC test, but can have a real effect on flame and fire test results. Consequently, the correlation of PCFC data with flame and fire test results is qualitative.

## References

- 1 R. E. Lyon, *Fire Materials*, 24 (2000) 179.
- 2 R. E. Lyon, R. N. Walters and S. I. Stolarov, *ASTM Inter.*, 3 (2006) 1.
- 3 V. Babrauskas, V. Babrauskas and S. Grayson, Eds., Elsevier Applied Science, pp. 207–223, 1992.
- 4 W. Thornton, *Philos. Mag. J. Sci.*, 33 (1917) 196.
- 5 C. Huggett, *Fire Mater.* 4 (1980) 61.
- 6 M. L. Janssens and W. J. Parker, *Oxygen Consumption Calorimetry, Heat Release in Fires*, V. Babrauskas and S. Grayson, eds., Elsevier Applied Science, pp. 31–59, 1992.
- 7 Standard Test Method for Heat and Visible Smoke Release Rates for Materials and Products Using an Oxygen Consumption Calorimeter, ASTM E 1354, American Society for Testing and Materials, West Conshohocken, PA.
- 8 Standard Test Method for Measurement of Synthetic Polymer Material Flammability Using a Fire Propagation Apparatus (FPA), ASTM E 2058, American Society for Testing and Materials, West Conshohocken, PA.
- 9 R. E. Lyon and R. N. Walters, *J. Anal. Appl. Pyrol.*, 71 (2004) 27.
- 10 W. M. Heffington, G. E. Parks, K. G. P. Sulzmann and S. S. Penner, *The Combustion Institute*, 1976, pp. 997–1010.
- 11 S. M. Reshetnikov and I. S. Reshetnikov, *Polym. Degrad. Stab.*, 64 (1999) 379.
- 12 P. R. Westmoreland, T. Inguilzian and K. Rotem, *Thermochm. Acta*, 67 (2001) 401.
- 13 R. E. Lyon, Ed. C. A. Harper, McGraw-Hill, NY, 2004, Chapter 3, pp. 1–51.
- 14 R. N. Walters and R. E. Lyon, *Flammability of Automotive Plastics*, Presented at the Society of

- Automotive Engineers (SAE) World Congress & Exposition, Detroit, MI, April 3–6, 2006.
- 15 R. E. Lyon and M. L. Janssens, Polymer Flammability, Encyclopedia of Polymer Science Engineering (on-line edition), John Wiley & Sons, New York, NY, October 2005.
  - 16 R. E. Lyon, Piloted Ignition of Combustible Solids, Society for the Advancement of Materials and Process Engineering (SAMPE) International Conference, Long Beach, CA, May 2–5, 2005.
  - 17 V. Babrauskas and R. D. Peacock, Fire Safety J., 18 (1992) 255.
  - 18 Standard Test Method for Heat and Visible Smoke Release Rates for Materials and Products, ASTM D 906, American Society for Testing and Materials, West Conshohocken, PA.
  - 19 Title 14 of the Code of Federal Regulations (CFR), Chapter 1, Federal Aviation Administration, Department of Transportation, Part 25, Airworthiness Standards: Transport Category Airplanes.
  - 20 Standard Test Method for Measuring the Minimum Oxygen Concentration to Support Candle-Like Combustion of Plastics (Oxygen Index), ASTM D 2863, American Society for Testing and Materials, West Conshohocken, PA.
  - 21 Flammability of Plastic Materials, UL 94 Section 2 (Horizontal: HB) and Section 3 (Vertical: V-0/1/2), Underwriters Laboratories Inc., Northbrook, IL, 1991
  - 22 R.E. Lyon, Fire & Flammability, Fire Risk & Hazard Assessment Research Symposium, Fire Protection Research Foundation, Baltimore, MD, July 9–11, 2003, pp. 22–32.
  - 23 V. Babrauskas, Ignition Handbook, Fire Science Publishers, Issaquah, WA, 2003.
  - 24 A. Tewarson, J. L. Lee and R. F. Pion, The Influence of Oxygen Concentration on Fuel Parameters for Fire Modeling, Eighteenth Symposium (International) on Combustion, The Combustion Institute, Pittsburgh, PA, pp. 563–570, 1981.

---

DOI: 10.1007/s10973-006-8257-z